frontiers in Chemistry

ORIGINAL RESEARCH
published: 27 June 2018
doi: 10.3389/fchem.2018.00255

Ag_3VO_4 Nanoparticles Decorated $Bi_2O_2CO_3$ Micro-Flowers: An Efficient Visible-Light-Driven Photocatalyst for the Removal of Toxic Contaminants

Shijie Li[1], Shiwei Hu[1], Wei Jiang[1], Yu Liu[1], Yanping Liu[2], Yingtang Zhou[1]*, Liuye Mo[1] and Jianshe Liu[3]*

[1] *Key Laboratory of Key Technical Factors in Zhejiang Seafood Health Hazards, Institute of Innovation & Application, Zhejiang Ocean University, Zhoushan, China,* [2] *Department of Environmental Engineering, Zhejiang Ocean University, Zhoushan, China,* [3] *State Environmental Protection Engineering Center for Pollution Treatment and Control in Textile Industry, College of Environmental Science and Engineering, Donghua University, Shanghai, China*

OPEN ACCESS

Edited by:
Junguang Tao,
Hebei University of Technology, China

Reviewed by:
Shiba Adhikari,
Oak Ridge National Laboratory (DOE), United States
Wenyao Li,
Shanghai University of Engineering Sciences, China

****Correspondence:***
Shijie Li
lishijie@zjou.edu.cn
Yingtang Zhou
zhouyingtang@zjou.edu.cn

Specialty section:
This article was submitted to Green and Sustainable Chemistry, a section of the journal Frontiers in Chemistry

Received: *14 May 2018*
Accepted: *08 June 2018*
Published: *27 June 2018*

Citation:
Li S, Hu S, Jiang W, Liu Y, Liu Y, Zhou Y, Mo L and Liu J (2018) Ag_3VO_4 Nanoparticles Decorated $Bi_2O_2CO_3$ Micro-Flowers: An Efficient Visible-Light-Driven Photocatalyst for the Removal of Toxic Contaminants. Front. Chem. 6:255. doi: 10.3389/fchem.2018.00255

Semiconductor-based photocatalysis is of great potential for tackling the environmental pollution. Herein, a novel hierarchical heterostructure of $Bi_2O_2CO_3$ micro-flowers *in-situ* decorated with Ag_3VO_4 nanoparticles was developed by a facile method. Various characterization techniques have been employed to study the physical and chemical property of the novel catalyst. The novel catalyst was utilized for the photocatalytic removal of industrial dyes (rhodamine B, methyl orange) and tetracycline antibiotic under visible-light irradiation. The results indicated that $Ag_3VO_4/Bi_2O_2CO_3$ heterojunctions showed a remarkably enhanced activity, significantly higher than those of bare Ag_3VO_4, $Bi_2O_2CO_3$, and the physical mixture of Ag_3VO_4 and $Bi_2O_2CO_3$ samples. This could be ascribed to an enhanced visible-light harvesting capacity and effective separation of charge carriers by virtue of the construction of hierarchical $Ag_3VO_4/Bi_2O_2CO_3$ heterojunction. Moreover, $Ag_3VO_4/Bi_2O_2CO_3$ also possesses an excellent cycling stability. The outstanding performance of $Ag_3VO_4/Bi_2O_2CO_3$ in removal of toxic pollutants indicates the potential of $Ag_3VO_4/Bi_2O_2CO_3$ in real environmental remediation.

HIGHLIGHTS

- Novel architectures of Ag_3VO_4 nanoparticles modified $Bi_2O_2CO_3$ micro-flowers were constructed.
- Novel $Ag_3VO_4/Bi_2O_2CO_3$ exhibited excellent photocatalytic activity and stability.
- $Ag_3VO_4/Bi_2O_2CO_3$ heterojunctions significantly promote the charge separation.

Keywords: Ag_3VO_4, $Bi_2O_2CO_3$, heterojunction, visible-light-driven, toxic pollutant removal

INTRODUCTION

Semiconductor photocatalysis has been regarded as one of the most promising nanotechnologies for the treatment of environmental pollution (Bora and Mewada, 2017; Cates, 2017; Wang W. et al., 2017; Zhang and Ma, 2017; Zhu and Wang, 2017). A significant research topic of photocatalysis is the exploration of highly active

photocatalysts (Li et al., 2014, 2017d, 2018b; Adhikari et al., 2015, 2016, 2017; Martin et al., 2015; Zhang et al., 2016, 2017; Mousavi et al., 2018; Yu et al., 2018).

The emergent $Bi_2O_2CO_3$ has attracted much interest for its good photocatalytic performance in the removal of toxic pollutants (Ni et al., 2016; Yu et al., 2018). However, the photocatalytic properties are still far from satisfactory owing to low solar utilization and fast recombination of electron-hole pairs. To improve the visible-light photocatalytic activity of $Bi_2O_2CO_3$, various strategies have been developed, such as design of microstructure (Zhao et al., 2011), deposition of metals (Yu et al., 2016), formation of heterojunction (Chen et al., 2016, 2017; Huang et al., 2016; Feng et al., 2017; Hu et al., 2017), and doping with ions (Dong et al., 2014; Xiong et al., 2015). The rational construction of heterojunctions can effectively ameliorate the visible-light absorption ability and significantly suppress the electron-hole recombination (Han et al., 2017; Li et al., 2017b,c,e; Zhong et al., 2018). The further development of novel $Bi_2O_2CO_3$-based catalysts is still required to offer more potential candidates for practical application and to figure out the reasons for the synergetic effect between the components.

Ag_3VO_4, an active VLD photocatalyst, has drawn much attention in virtue of its unique band structures. Ag_3VO_4 has been coupled with other semiconductors (e.g., Bi_2WO_6 Li et al., 2017a; Zhang and Ma, 2017, BiOI Wang et al., 2015, BiOCl Wang et al., 2016, C_3N_4 Wang et al., 2014, $BiVO_4$ Yan et al., 2016a, WO_3 Yan et al., 2016b) to fabricate high-performance photocatalysts. To date, researches on Ag_3VO_4 nanoparticles decorated $Bi_2O_2CO_3$ micro-flowers for the visible-light photodegradation of toxic contaminants have not been reported.

Herein, we report Ag_3VO_4 nanoparticles evenly deposited on the surface of $Bi_2O_2CO_3$ micro-flowers by a simple precipitation method. Ag_3VO_4 nanoparticles can optimize the visible-light response and facilitate the separation of charge carriers, endowing the novel heterojunction with excellent visible-light photocatalytic performance. The plausible visible-light photocatalysis mechanism of $Ag_3VO_4/Bi_2O_2CO_3$ is also proposed.

EXPERIMENT

Chemicals

Bismuth citrate ($BiO_7C_6H_5$), sodium carbonate (Na_2CO_3), ethanol (CH_3CH_2OH), silver nitrate ($AgNO_3$), sodium vanadate (Na_3VO_4), rhodamine B (RhB), ammonium oxalate (AO), $AgNO_3$, tetracycline hydrochloride (TC), *p*-benzoquinone (BQ), methyl orange (MO), and iso-propanol (IPA) were bought from Shanghai Chemical Reagent factory (China). All the reagents were analytic grade and used without further treatment.

Synthesis of Catalysts

$Bi_2O_2CO_3$ was synthesized via a hydrothermal procedure. Briefly, 2 mmol of sodium carbonate (Na_2CO_3) and 2 mmol of bismuth citrate ($BiO_7C_6H_5$) were sequentially dissolved in the solution containing 30 mL of deionized water and 5 mL of absolute ethanol with the assistance of ultra-sonication. The resulting solution was sealed in a 50 mL autoclave and heated at 160°C for 25 h. After the reactor system was cooled down, the precipitants were washed thoroughly with de-ionized water and dried at 80°C overnight.

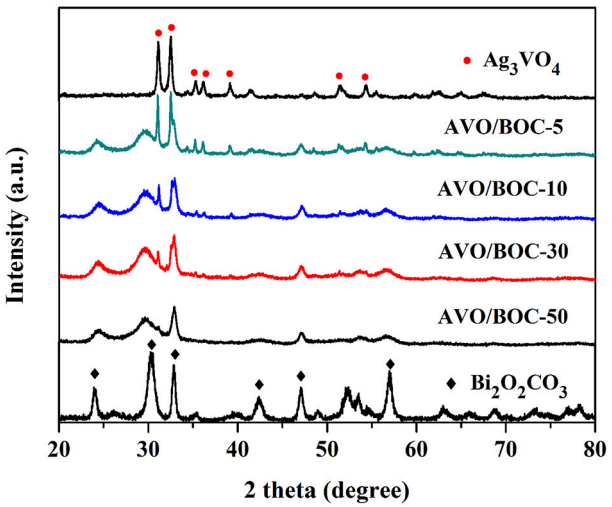

FIGURE 1 | XRD patterns of $Ag_3VO_4/Bi_2O_2CO_3$ heterojunctions (AVO/BOC-5, AVO/BOC-10, AVO/BOC-30, and AVO/BOC-50), pure $Bi_2O_2CO_3$, and Ag_3VO_4.

$Ag_3VO_4/Bi_2O_2CO_3$ heterojunctions were constructed by a simple precipitation method. Briefly, an appropriate amount of $Bi_2O_2CO_3$ was ultrasonically suspended in 50 mL of H_2O. Then, 3 mmol $AgNO_3$ was dissolved in the above solution under magnetical stirring. After that, Na_3VO_4 (20 mL, 0.05 mol L^{-1}) solution was slowly dropped into the mixture with vigorous stirring for 5 h. Lastly, the obtained solids were washed with deionized water four times and dried at 80°C for 10 h to get the $Ag_3VO_4/Bi_2O_2CO_3$ heterojunctions. The heterojunctions with different $Bi_2O_2CO_3/Ag_3VO_4$ weight ratios of 0.05/1, 0.10/1, 0.30/1, and 0.50/1 are labeled as AVO/BOC-5, AVO/BOC-10, AVO/BOC-30, and AVO/BOC-50, respectively. Ag_3VO_4 was prepared in the absence of $Bi_2O_2CO_3$.

Characterization of Catalysts

The scanning electron microscopy (SEM, Hitachi S-4800) and transmission electron microscopy (TEM, JEM-2100 JEOL) were applied to characterize the morphology of the samples. Bruker Quantax 400 energy-dispersive X-ray spectroscopy (EDS) was used to identify the chemical composition. Powder X-ray diffractometer (XRD, MSAL XD2) was used to get the XRD patterns of the samples. UV–Vis diffuse reflectance spectra (DRS) were obtained on a spectrophotometer (Shimadzu UV−2600). Photoluminescence (PL) spectra of the samples were recorded on a Hitachi RF-6000 spectrophotometer.

Photocatalytic Tests

Pollutant [rhodamine B (RhB), methyl orange (MO), and tetracycline hydrochloride (TC)] removal performances were tested under visible-light irradiation, 300 W xenon lamp with filter ($\lambda > 400$ nm). The photocatalytic reaction was conducted

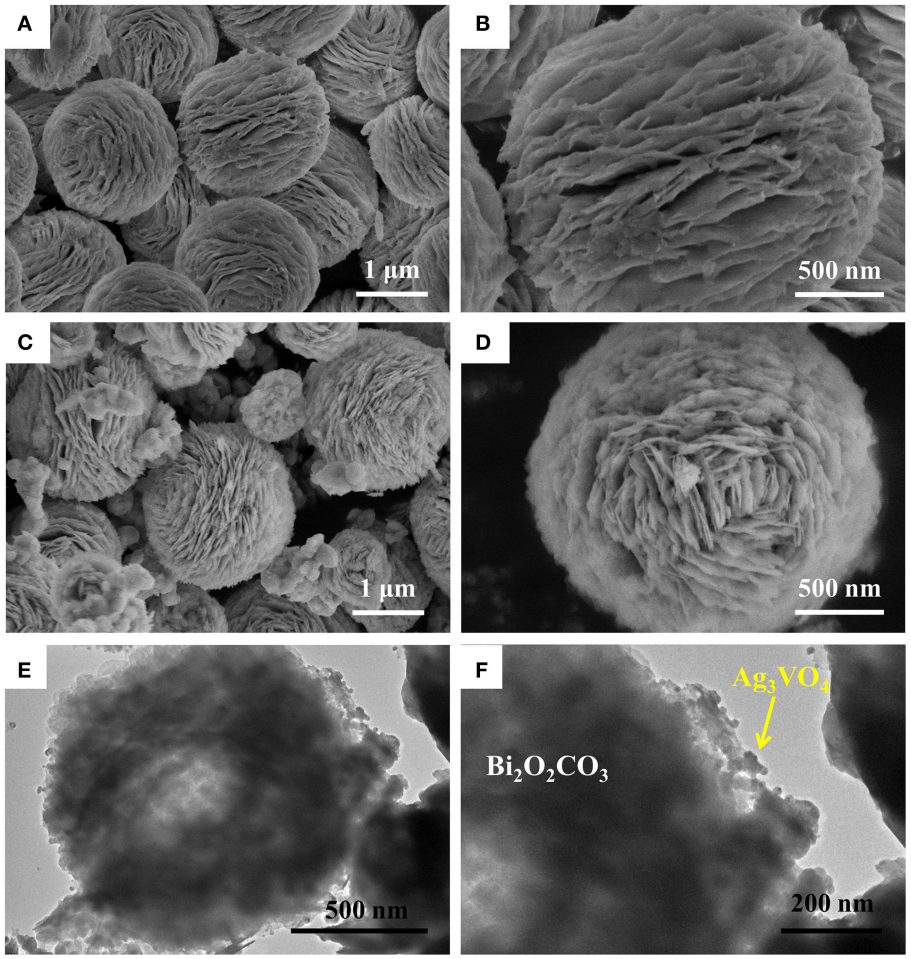

FIGURE 2 | SEM images of pristine $Bi_2O_2CO_3$ **(A,B)** and AVO/BOC-30 **(C,D)**; TEM images of AVO/BOC-10 **(E,F)**.

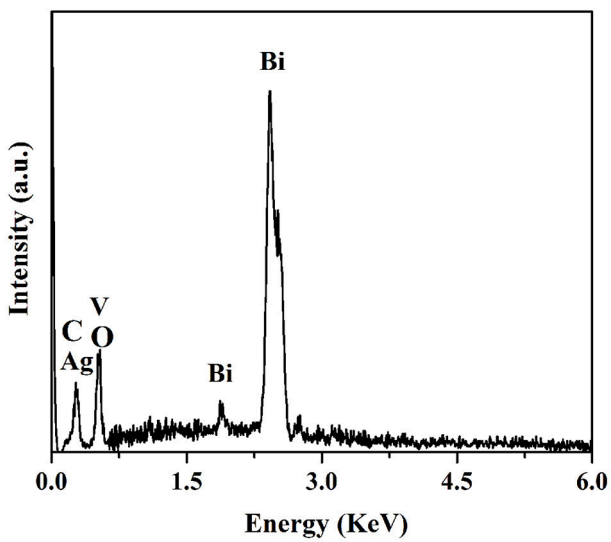

FIGURE 3 | EDS spectra of AVO/BOC-10.

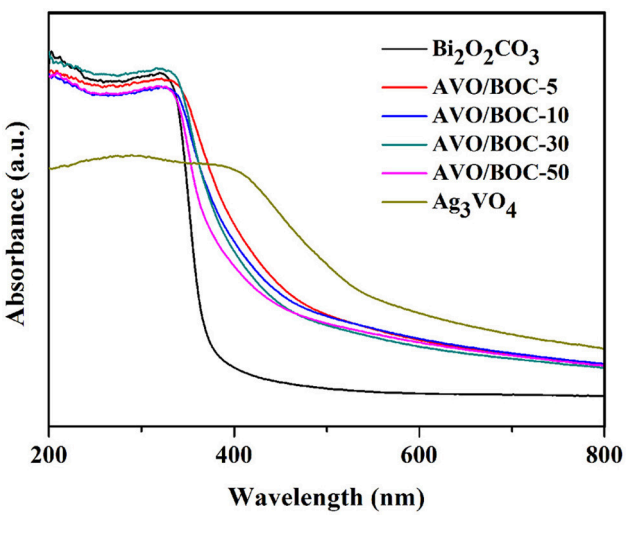

FIGURE 4 | The UV–Vis DRS of bare $Bi_2O_2CO_3$, Ag_3VO_4 and $Ag_3VO_4/Bi_2O_2CO_3$ heterojunctions.

in a glass reactor containing 80 mL of RhB (5 mg L^{-1}), MO (5 mg L^{-1}), or TC (20 mg L^{-1}) solution, and 40 mg of catalyst. The solution was first ultrasonically dispersed for 1 min and then magnetically stirred in the dark for 1 h. 1.5 mL of solution was taken at specified time, and centrifuged to remove the solids. The pollutant concentrations were determined using a Shimadzu UV-2600 spectrophotometer. Total organic carbon (TOC) value of the pollutant solutions during reaction was detected on a Shimadzu TOC analyzer.

RESULTS AND DISCUSSION

Characterization

Figure 1 displays the XRD patterns of the as-prepared pure Ag_3VO_4, $Bi_2O_2CO_3$, and their heterojunctions (AVO/BOC-5, AVO/BOC-10, AVO/BOC-30, and AVO/BOC-50). The diffraction peaks of Ag_3VO_4 and $Bi_2O_2CO_3$ prepared match well with monoclinic phase of Ag_3VO_4 (JCPDS 43-0542) and tetragonal phase of $Bi_2O_2CO_3$ (JCPDS 41-1488), respectively.

When a small amount of Ag_3VO_4 was introduced, no diffraction peaks of Ag_3VO_4 can be observed in the XRD pattern of AVO/BOC-50. As the Ag_3VO_4 content increases, AVO/BOC-30, AVO/BOC-10, and AVO/BOC-5 show the diffraction peaks of both $Bi_2O_2CO_3$ and Ag_3VO_4, indicating the successful fabrication of $Ag_3VO_4/Bi_2O_2CO_3$ heterojunctions.

The microstructures of $Bi_2O_2CO_3$ and $Ag_3VO_4/Bi_2O_2CO_3$ heterojunctions were investigated by using SEM. The SEM images in **Figures 2A,B** show that the obtained $Bi_2O_2CO_3$ exhibits flower-like microspheres constructed by countless nano-plates (Zhao et al., 2011). The SEM images in **Figures 2C,D** show the representative AVO/BOC-10 also possesses sphere-like morphology as that for pure $Bi_2O_2CO_3$. Of note, numerous Ag_3VO_4 nanoparticles were deposited on the surfaces of AVO/BOC-10.

The more detailed microstructures of AVO/BOC-10 were studied by TEM. As shown in **Figures 2E,F,** AVO/BOC-10 consists of $Bi_2O_2CO_3$ micro-flower (diameter: ~1.1 μm) and Ag_3VO_4 nanoparticles (size: ~26 nm), and they were tightly combined with each other to generate closely hybrid hetero-structure, in favor of transfer and separation of charge carriers (Huang et al., 2015; Zhang et al., 2016; Li et al., 2017a).

The corresponding EDS spectra of AVO/BOC-10 revealed that only signals for Ag, V, Bi, C, and O elements were detected, indicating the high purity of the sample (**Figure 3**). The above results verified that the facile precipitation method could successfully fabricate $Ag_3VO_4/Bi_2O_2CO_3$ heterojunctions with intimate contact between two constituents.

The sunlight absorption capability and band structures of a photocatalyst usually exert a significant effect on its photocatalytic performance. Thus, the UV–Vis DRS spectra of bare $Bi_2O_2CO_3$, Ag_3VO_4, and $Ag_3VO_4/Bi_2O_2CO_3$ heterojunctions are measured and illustrated in **Figure 4**. $Bi_2O_2CO_3$ exhibited a strong absorption in the UV region with the absorption edge at 385 nm, in accordance with the previous

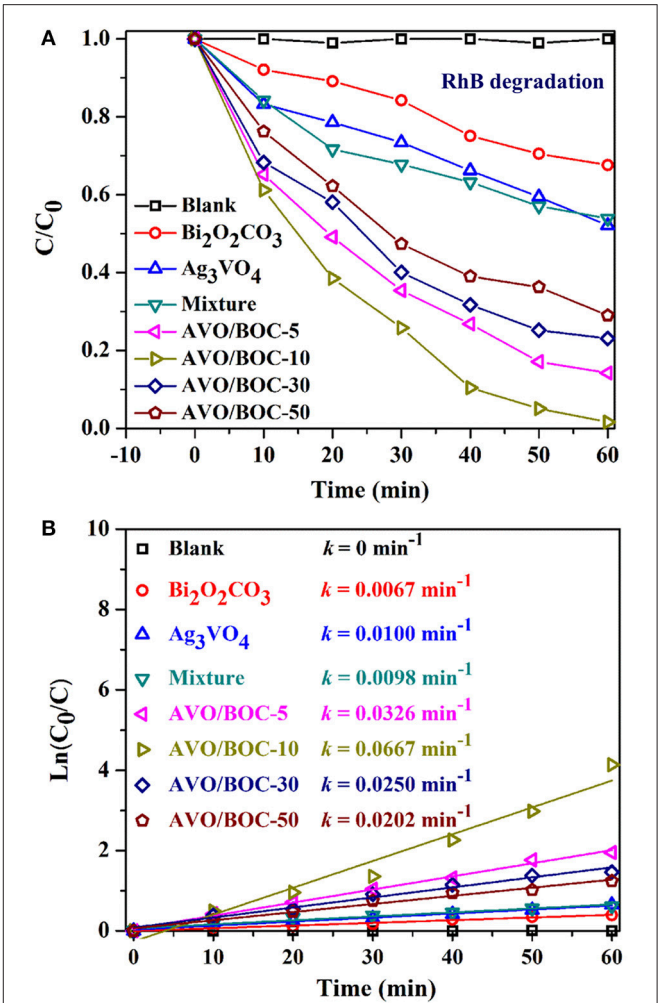

FIGURE 5 | (A) Photocatalytic degradation efficiency of RhB over different catalysts under visible light. **(B)** Rate constants of RhB degradation during reaction over different catalysts.

reports (Zhao et al., 2011; Hu et al., 2017). Ag_3VO_4 performed a 575 nm absorption edge in the VL region, consistent with the reported values (Wang et al., 2015; Yan et al., 2016b; Li et al., 2017a). Intriguingly, the combination of Ag_3VO_4 and $Bi_2O_2CO_3$ substantially ameliorated the VL absorption properties of the heterojunctions, which is beneficial for the effective utilization of solar energy.

The bandgap width (Eg) was estimated according to the equation: Eg = 1240/λg (eV), and the Eg value of Ag_3VO_4 and $Bi_2O_2CO_3$ are about 2.15 and 3.23 eV. The band positions (E_{VB} and E_{CB}) of Ag_3VO_4 and $Bi_2O_2CO_3$ can be calculated using the following formula:

$$E_{VB} = X - E^e + 0.5E_g \quad (1)$$

$$E_{CB} = E_{VB} - E_g \quad (2)$$

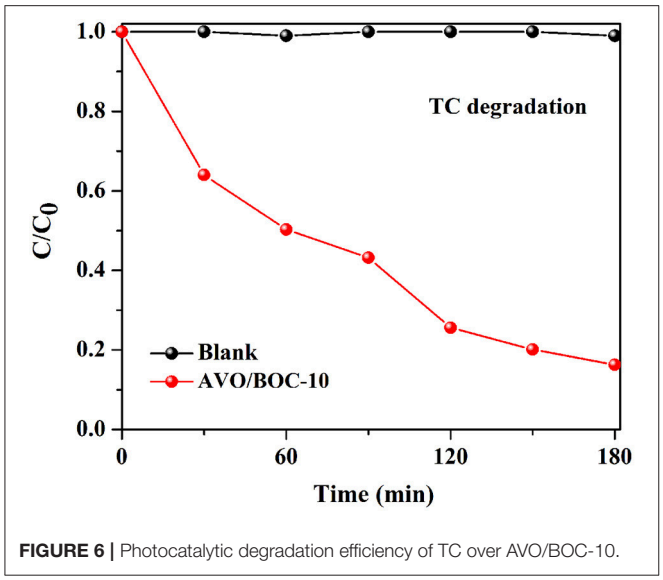

FIGURE 6 | Photocatalytic degradation efficiency of TC over AVO/BOC-10.

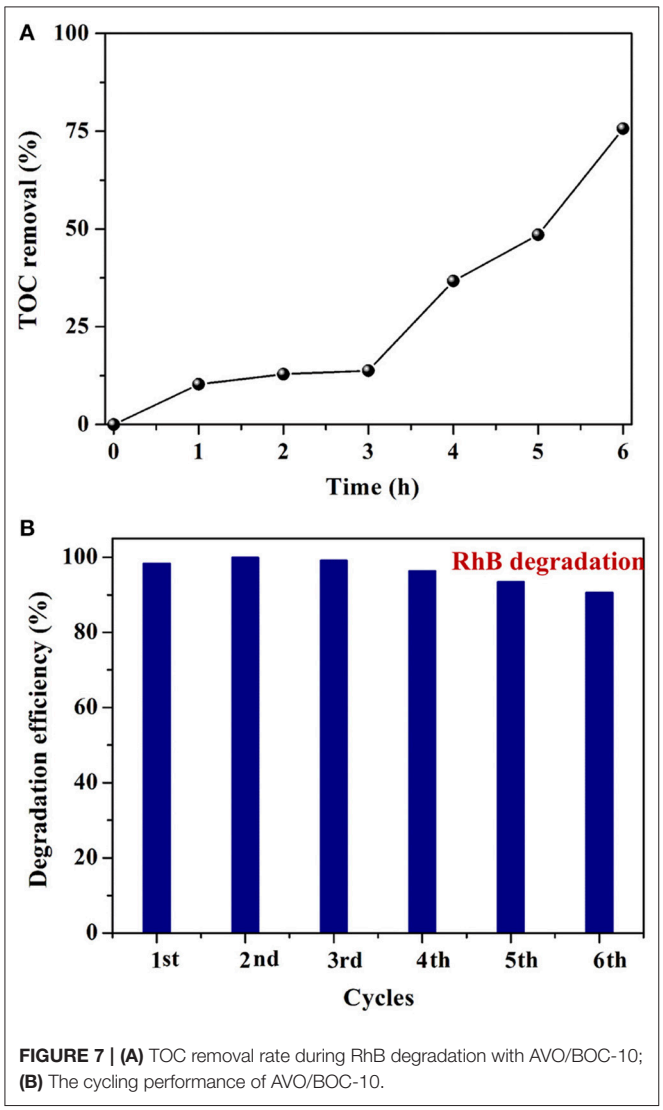

FIGURE 7 | (A) TOC removal rate during RhB degradation with AVO/BOC-10; **(B)** The cycling performance of AVO/BOC-10.

Where X [ca. 6.36 eV for Ag_3VO_4 (Li et al., 2017a), and ca. 6.54 eV for $Bi_2O_2CO_3$ Liang et al., 2014] is the electronegativity of the semiconductor. E^e value equals to ∼4.5 eV. On the basis of above data, the E_{VB} and E_{CB} of Ag_3VO_4 were determined as 0.01 and 2.14 eV, while those of $Bi_2O_2CO_3$ were 0.2 and 3.53 eV.

Photocatalytic Property

The VLD photocatalytic activity of $Ag_3VO_4/Bi_2O_2CO_3$ heterojunctions was studied through the degradation of RhB (**Figure 5**), MO (Figure S1), and TC (**Figure 6**). **Figure 5A** displays the concentration change of RhB dye solution under visible light with the as-prepared catalysts. The blank test conducted without the presence of catalyst showed that RhB was not degraded after 60 min of irradiation. The photocatalytic activity of pristine $Bi_2O_2CO_3$ is much lower than other samples and the RhB degradation efficiency is 31.4%, mainly due to its large bandgap (Yu et al., 2016). Only 49.8% of RhB was removed by pure Ag_3VO_4 due to the high recombination rate of charge carriers (Yan et al., 2016b). Inspiringly, when $Bi_2O_2CO_3$ was decorated with Ag_3VO_4, the catalytic activity of these heterojunctions was substantially improved. After 60 min of irradiation, the RhB degradation efficiencies by using AVO/BOC-5, AVO/BOC-10, AVO/BOC-30 and AVO/BOC-50 were 85.8, 98.4, 76.9, and 71.1%, respectively, much higher than that by using the pristine $Bi_2O_2CO_3$, Ag_3VO_4, or the mechanical mixture (91 wt% Ag_3VO_4 + 9 wt% $Bi_2O_2CO_3$). The activity of $Ag_3VO_4/Bi_2O_2CO_3$ increases gradually and then declines regularly, while AVO/BOC-10 has the highest photocatalytic activity, indicating the vital role of Ag_3VO_4 in enhancing the activity.

The degradation rate constants (k) of RhB were presented in **Figure 5B**. The photocatalytic activity of AVO/BOC-10 achieved the maximum value of $k = 0.0667\ min^{-1}$, it was about 8.9, 5.7, and 5.8-folds higher than pure $Bi_2O_2CO_3$ (0.0067 min^{-1}), Ag_3VO_4 (0.0100 min^{-1}), and the mechanical mixture (0.0098 min^{-1}).

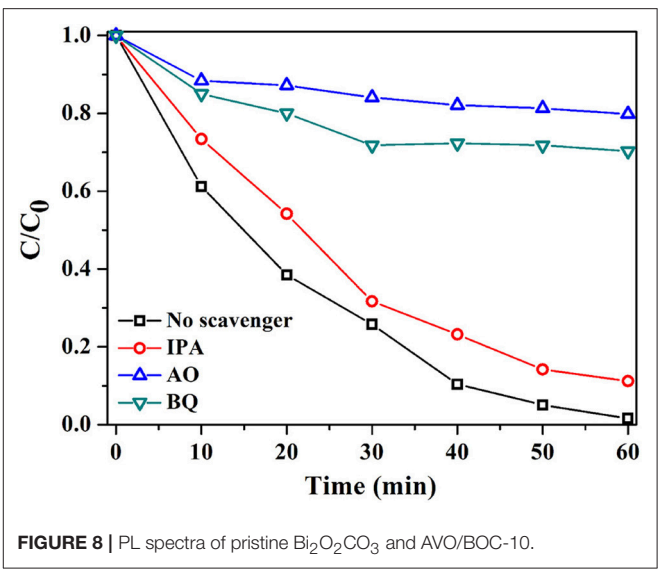

FIGURE 8 | PL spectra of pristine $Bi_2O_2CO_3$ and AVO/BOC-10.

The degradation of antibiotic TC or industrial dye MO was also performed to further test the VL photocatalysis of AVO/BOC-10 (**Figure 6** and Figure S1). Apparently, AVO/BOC-10 also showed high activity in the degradation of TC and MO (Figure S1). The TC or MO degradation efficiency with AVO/BOC-10 as the catalyst was 83.7 or 94.2% after 180 min of reaction. These results demonstrate that AVO/BOC-10 exhibits extraordinary photocatalytic activity in the removal of toxic pollutants.

To assess the mineralization capability of $Ag_3VO_4/Bi_2O_2CO_3$, the TOC data during RhB (50 mg L^{-1}) degradation over AVO/BOC-10 (200 mg) was recorded and analyzed (**Figure 7A**). It is found that the TOC removal efficiency of RhB with AVO/BOC-10 is 76.4% after 6 h of reaction, suggesting that AVO/BOC-10 possesses strong mineralization ability during the photocatalytic reaction.

For evaluating the stability of $Ag_3VO_4/Bi_2O_2CO_3$, six successive cycles of RhB degradation with AVO/BOC-10 as a catalyst were carried out. Inspiringly, no apparent loss of activity of the catalyst in six times of reuse was observed, and the RhB removal efficiency retained 92.1% in the sixth run (**Figure 7B**). In addition, the catalyst before and after six runs was characterized by XRD technique (Figure S2), and no obvious changes in the crystalline phases was detected, verifying the good stability of AVO/BOC-10. Moreover, the cycling degradation involving TC antibiotic further confirms the good stability of AVO/BOC-10 (Figure S3). The photocatalytic tests demonstrate that AVO/BOC-10 endowed with high activity and stability is a kind of promising VLD photocatalysts, exhibiting great potential for wastewater treatment.

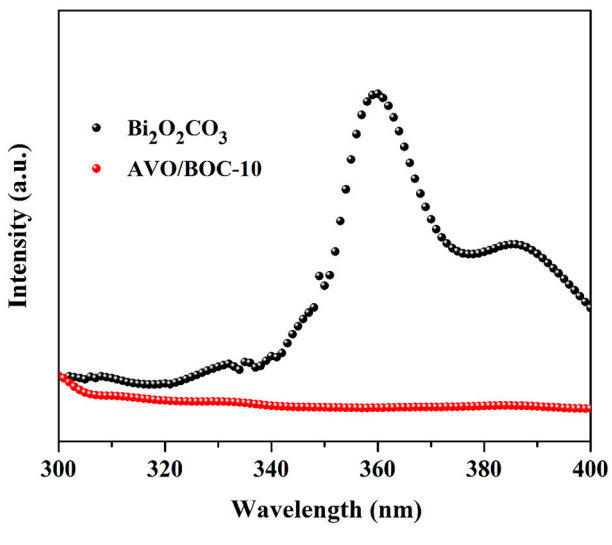

FIGURE 9 | Radical scavenge tests with AVO/BOC-10 as the catalyst.

Origin of the Improved Performance

The photocatalytic activity depends strongly on the separation efficiency of photo-induced charge carriers (Hu et al., 2017; Li et al., 2017a), thus, photoluminescence (PL) spectrum of the samples were acquired to illustrate the electron-hole separation (**Figure 8**). Apparently, the PL intensity of AVO/BOC-10 is much weaker than that of pristine $Bi_2O_2CO_3$. Since a weaker PL intensity signifies higher separation rate of charge carriers, AVO/BOC-10 should possess a higher separation efficiency compared with $Bi_2O_2CO_3$. That is to say, the photo-induced electron-hole pairs were efficiently separated in AVO/BOC-10 system due to

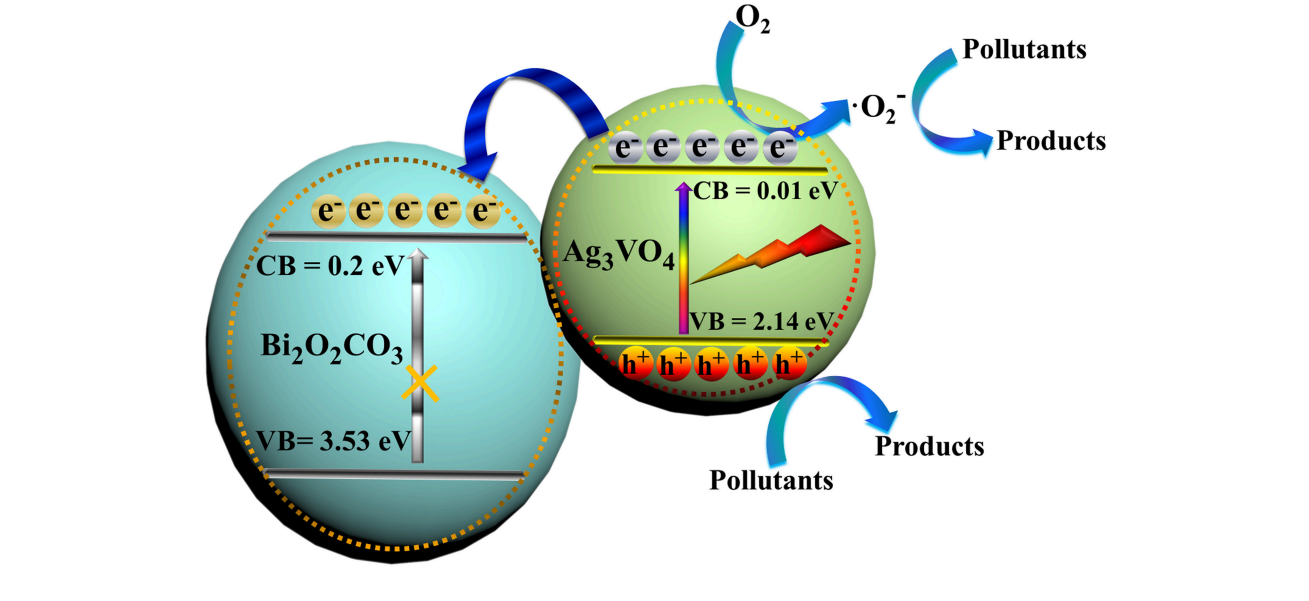

FIGURE 10 | Photocatalytic degradation mechanism of toxic pollutant over $Ag_3VO_4/Bi_2O_2CO_3$.

the interfacial charge transfer, resulting in the elevated photocatalytic activity.

For mechanistic study, various additives were employed to research the main active species in the photocatalytic reaction process (**Figure 9**) (Zhang and Ma, 2017; Li et al., 2018). When 1 mmol of BQ (benzoquinone, $O_2^{\bullet-}$ scavenger) or AO (ammonium oxalate, h^+ scavenger) was introduced, the activity of AVO/BOC-10 was substantially quenched, and the RhB degradation efficiency declined from 98.4 to 29.7% or 20.2%, revealing that $O_2^{\bullet-}$ and h^+ should play vital roles in the photocatalysis. On the contrary, no obvious decrease in the activity was observed with adding 1 mmol of IPA (isopropyl alcohol, •OH scavenger), signifying that •OH plays a minor role.

Based on this systematic investigation, a possible visible-light photocatalytic mechanism for pollutant degradation over $Ag_3VO_4/Bi_2O_2CO_3$ is proposed (**Figure 10**). Apparently, the position of CB and VB between Ag_3VO_4 and $Bi_2O_2CO_3$ are beneficial to achieve effective separation of photo-generated charge carriers (Wang F. F. et al., 2017; Ye et al., 2018). Photo-generated electrons and holes are produced on Ag_3VO_4 under visible-light illumination. Since the CB of $Bi_2O_2CO_3$ is lower than that of Ag_3VO_4, the electrons can be injected readily from Ag_3VO_4 to $Bi_2O_2CO_3$. The electrons on the CB of $Bi_2O_2CO_3$ can react with O_2 to form active $O_2^{\bullet-}$, degrading toxic pollutants such as RhB/MO/TC. Simultaneously, the holes with strong oxide capability in the VB of Ag_3VO_4 are available to take part in the decomposition of pollutants. In such a way, the electrons and holes can be effectively utilized, as evidenced by the result of PL spectra of $Bi_2O_2CO_3$ and $Ag_3VO_4/Bi_2O_2CO_3$ (**Figure 8**). In summary, the combination of Ag_3VO_4 and $Bi_2O_2CO_3$ enhances the charge separation, leading to the high activity.

CONCLUSIONS

In this study, innovative $Ag_3VO_4/Bi_2O_2CO_3$ heterojunction photocatalysts were synthesized *via* a simple procedure. The $Ag_3VO_4/Bi_2O_2CO_3$ heterojunction (AVO/BOC-10) displayed the optimal photocatalytic properties toward the degradation of toxic pollutants (RhB dye, MO dye, and TC antibiotic), much higher than pristine $Bi_2O_2CO_3$ and Ag_3VO_4. The close contact and the match of bandgap structure between both constituents boost the separation of electron-hole pairs, mainly accounting for the activity enhancement. The holes and $O_2^{\bullet-}$ were determined as the primary active species responsible for the efficient removal and mineralization of the toxic pollutants. Therefore, $Ag_3VO_4/Bi_2O_2CO_3$ holds huge potential for real wastewater treatment.

AUTHOR CONTRIBUTIONS

SL designed and performed the experiments, and data analysis. SH, WJ, YuL, YaL, YZ, JL, and LM assisted with some of the tests. SL wrote the main content of the paper. All authors have read and approved the paper to be submitted.

ACKNOWLEDGMENTS

This work has been financially supported by the National Natural Science Foundation of China (51708504 and 31501573), the Public Projects of Zhejiang Province (2017C32079 and LGN18E080003), the Science and Technology Project of Zhoushan (2017C41006, 2016C41012, 2015C21014, and 2015C21013), the National Key Research Development Program of China (2016YFC0400501), and the Research Startup Foundation of Zhejiang Ocean University (12215090117).

SUPPLEMENTARY MATERIAL

The Supplementary Material for this article can be found online at: https://www.frontiersin.org/articles/10.3389/fchem.2018.00255/full#supplementary-material

REFERENCES

Adhikari, S. P., Dean, H., Hood, Z. D., Peng, R., More, K. L., Ivanov, I., et al. (2015). Visible-light-driven Bi2O3/WO3 composites with enhanced photocatalytic activity. *RSC Adv.* 5, 91094–91102. doi: 10.1039/C5RA13579F

Adhikari, S. P., Hood, Z. D., More, K. L., Chen, V. W., and Lachgar, A. (2016). A visible-light-active heterojunction with enhanced photocatalytic hydrogen generation. *ChemSusChem* 9, 1869–1879. doi: 10.1002/cssc.201600424

Adhikari, S. P., Hood, Z. D., Wang, H., Peng, R., Krall, A., Li, H., et al. (2017). Enhanced visible light photocatalytic water reduction from a g-C3N4/SrTa2O6 heterojunction. *Appl. Catal. B* 217, 448–458. doi: 10.1016/j.apcatb.2017.05.092

Bora, L. V., and Mewada, R. K. (2017). Visible/solar light active photocatalysts for organic effluent treatment: fundamentals, mechanisms and parametric review. *Renew. Sustain. Energy Rev.* 76, 1391–1421. doi: 10.1016/j.rser.2017.01.130

Cates, E. L. (2017). Photocatalytic water treatment: so where are we going with this? *Environ. Sci. Technol.* 51, 757–758. doi: 10.1021/acs.est.6b06035

Chen, J. L., Li, S. J., Hu, S. W., and Jiang, W. (2017). Enhanced visible-light photocatalytic activity of Ag/AgI coupled $Bi_2O_2CO_3$ microspheres. *Mater. Lett.* 191, 123–127. doi: 10.1016/j.matlet.2016.12.096

Chen, J., Mei, W. G., Huang, Q. J., Chen, N. N., Lu, C. L., Zhu, H. J., et al. (2016). Highly efficient three-dimensional flower-like $AgI/Bi_2O_2CO_3$ heterojunction with enhanced photocatalytic performance. *J. Alloys Compd.* 688, 225–234. doi: 10.1016/j.jallcom.2016.07.196

Dong, F., Xiong, T., Wang, R., Sun, Y. J., and Jiang, Y. K. (2014). Growth mechanism and photocatalytic activity of self-organized N-doped $(BiO)_2CO_3$ hierarchical nanosheet microspheres from bismuth citrate and urea. *Dalton Trans.* 43, 6631–6642. doi: 10.1039/c3dt53383b

Feng, X., Zhang, W., Sun, Y., Huang, H., and Dong, F. (2017). Fe(III) cluster-grafted $(BiO)_2CO_3$ superstructures: in situ DRIFTS investigation on IFCT-enhanced visible light photocatalytic NO oxidation. *Environ. Sci. Nano* 4, 604–612. doi: 10.1039/c6en00637j

Han, W., Li, Z., Li, Y., Fan, X., Zhang, F., Zhang, G., et al. (2017). The promoting role of different carbon allotropes cocatalysts for semiconductors in photocatalytic energy generation and pollutants degradation. *Front. Chem.* 5:84. doi: 10.3389/fchem.2017.00084

Hu, J., Chen, D., Li, N., Xu, Q., Li, H., He, J., et al. (2017). *In situ* fabrication of $Bi_2O_2CO_3/MoS_2$ on carbon nanofibers for efficient photocatalytic removal

of NO under visible-light irradiation. *Appl. Catal. B* 217, 224–231. doi: 10.1016/j.apcatb.2017.05.088

Huang, H. W., He, Y., Du, X., Chu, P. K., and Zhang, Y. H. (2015). A general and facile approach to heterostructured core/Shell $BiVO_4$/BiOI p-n junction: room-temperature *in situ* assembly and highly boosted visible-light photocatalysis. *ACS Sust. Chem. Eng.* 3, 3262–3273. doi: 10.1021/acssuschemeng.5b01038

Huang, Y. C., Fan, W. J., Long, B., Li, H. B., Zhao, F. Y., Liu, Z. L., et al. (2016). Visible light $Bi_2S_3/Bi_2O_3/Bi_2O_2CO_3$ photocatalyst for effective degradation of organic pollutions. *Appl. Catal. B* 185, 68–76. doi: 10.1016/j.apcatb.2015.11.043

Li, S., Hu, S., Jiang, W., Liu, Y., Liu, Y., Zhou, Y., et al. (2018). Ag_2WO_4 nanorods decorated with AgI nanoparticles: novel and efficient visible-light-driven photocatalysts for the degradation of water pollutants. *Beilstein J. Nanotechnol.* 9, 1308–1316. doi: 10.3762/bjnano.9.123

Li, S. J., Hu, S. W., Jiang, W., Liu, Y., Liu, J. S., and Wang, Z. H. (2017a). Facile synthesis of flower-like Ag_3VO_4/Bi_2WO_6 heterojunction with enhanced visible-light photocatalytic activity. *J. Colloid Interface Sci.* 501, 156–163. doi: 10.1016/j.jcis.2017.04.057

Li, S. J., Hu, S. W., Jiang, W., Liu, Y., Liu, J. S., and Wang, Z. H. (2017b). Synthesis of n-type TaON microspheres decorated by p-type Ag_2O with enhanced visible light photocatalytic activity. *Mol. Catal.* 435, 135–143. doi: 10.1016/j.mcat.2017.03.027

Li, S. J., Hu, S. W., Jiang, W., Liu, Y. P., Zhou, Y. T., Liu, Y., et al. (2018b). Hierarchical architectures of bismuth molybdate nanosheets onto nickel titanate nanofibers: facile synthesis and efficient photocatalytic removal of tetracycline hydrochloride. *J. Colloid Interface Sci.* 521, 42–49. doi: 10.1016/j.jcis.2018.03.033

Li, S. J., Hu, S. W., Xu, K. B., Jiang, W., Liu, J. S., and Wang, Z. H. (2017c). A novel heterostructure of BiOI nanosheets anchored onto MWCNTs with excellent visible-light photocatalytic activity. *Nanomaterials* 7, 22–34. doi: 10.3390/nano7010022

Li, S. J., Hu, S. W., Zhang, J. L., Jiang, W., and Liu, J. S. (2017d). Facile synthesis of Fe_2O_3 nanoparticles anchored on Bi_2MoO_6 microflowers with improved visible light photocatalytic activity. *J. Colloid Interface Sci.* 497, 93–101. doi: 10.1016/j.jcis.2017.02.069

Li, S. J., Shen, X. F., Liu, J. S., and Zhang, L. S. (2017e). Synthesis of Ta_3N_5/Bi_2MoO_6 core-shell fiber-shaped heterojunctions as efficient and easily recyclable photocatalysts. *Environ. Sci. Nano* 4, 1155–1167. doi: 10.1039/C6EN00706F

Li, S. J., Zhang, L. S., Wang, H. L., Chen, Z. G., Hu, J. Q., Xu, K. B., et al. (2014). Ta3N5-Pt nonwoven cloth with hierarchical nanopores as efficient and easily recyclable macroscale photocatalysts. *Sci. Rep.* 4:3978. doi: 10.1038/srep03978

Liang, N., Wang, M., Jin, L., Huang, S. S., Chen, W. L., Xu, M., et al. (2014). Highly efficient $Ag_2O/Bi2O_2CO_3$ p-n heterojunction photocatalysts with improved visible-light responsive activity. *ACS Appl. Mater. Interfaces* 6, 11698–11705. doi: 10.1021/am502481z

Martin, D. J., Liu, G., Moniz, S. J. A., Bi, Y., Beale, A. M., Ye, J., et al. (2015). Efficient visible driven photocatalyst, silver phosphate: performance, understanding and perspective. *Chem. Soci. Rev.* 44, 7808–7828. doi: 10.1039/c5cs00380f

Mousavi, M., Habibi-Yangjeh, A., and Pouran, S. R. (2018). Review on magnetically separable graphitic carbon nitride-based nanocomposites as promising visible-light-driven photocatalysts. *J. Mater. Sci. Mater. Electron.* 29, 1719–1747. doi: 10.1007/s10854-017-8166-x

Ni, Z. L., Sun, Y. J., Zhang, Y. X., and Dong, F. (2016). Fabrication, modification and application of $(BiO)_2CO_3$-based photocatalysts: a review. *Appl. Surf. Sci.* 365, 314–335. doi: 10.1016/j.apsusc.2015.12.231

Wang, F. F., Li, Q., and Xu, D. S. (2017). Recent progress in semiconductor-based nanocomposite photocatalysts for solar-to-chemical energy conversion. *Adv. Energy Mater.* 7:1700529. doi: 10.1002/aenm.201700529

Wang, P. F., Tang, H., Ao, Y. H., Wang, C., Hou, J., Qian, J., et al. (2016). *In-situ* growth of Ag_3VO_4 nanoparticles onto BiOCl nanosheet to form a heterojunction photocatalyst with enhanced performance under visible light irradiation. *J. Alloys Compd.* 688, 1–7. doi: 10.1016/j.jallcom.2016.07.180

Wang, S. M., Guan, Y., Wang, L. P., Zhao, W., He, H., Xiao, J., et al. (2015). Fabrication of a novel bifunctional material of $BiOI/Ag_3VO_4$ with high adsorption-photocatalysis for efficient treatment of dye wastewater. *Appl. Catal. B* 168–169, 448-457. doi: 10.1016/j.apcatb.2014.12.047

Wang, S. M., Li, D. L., Sun, C., Yang, S. G., Guan, Y., and He, H. (2014). Synthesis and characterization of $g\text{-}C_3N_4/Ag_3VO_4$ composites with significantly enhanced visible-light photocatalytic activity for triphenylmethane dye degradation. *Appl. Catal. B* 144, 885–892. doi: 10.1016/j.apcatb.2013.08.008

Wang, W., Li, G., Xia, D., An, T., Zhao, H., and Wong, P. K. (2017). Photocatalytic nanomaterials for solar-driven bacterial inactivation: recent progress and challenges. *Environ. Sci. Nano* 4, 782–799. doi: 10.1039/C7EN00063D

Xiong, T., Huang, H. W., Sun, Y. J., and Dong, F. (2015). *In situ* synthesis of a C-doped $(BiO)_2CO_3$ hierarchical self-assembly effectively promoting visible light photocatalysis. *J. Mater. Chem. A* 3, 6118–6127. doi: 10.1039/c5ta00103j

Yan, M., Wu, Y. L., Yan, Y., Yan, X., Zhu, F. F., Hua, Y. Q., et al. (2016a). Synthesis and characterization of novel $BiVO_4/Ag_3VO_4$ heterojunction with enhanced visible-light-driven photocatalytic degradation of dyes. *ACS Sustainable Chem. Eng.* 4, 757–766. doi: 10.1021/acssuschemeng.5b00690

Yan, M., Wu, Y. L., Zhu, F. F., Hua, Y. Q., and Shi, W. D. (2016b). The fabrication of a novel Ag_3VO_4/WO_3 heterojunction with enhanced visible light efficiency in the photocatalytic degradation of TC. *Phys. Chem. Chem. Phys.* 18, 3308–3315. doi: 10.1039/c5cp05599g

Ye, R., Zhao, J., Wickemeyer, B. B., Toste, F. D., and Somorjai, G. A. (2018). Foundations and strategies of the construction of hybrid catalysts for optimized performances. *Nat. Catal.* 1, 318–325. doi: 10.1038/s41929-018-0052-2

Yu, C. L., Zhou, W. Q., Zhu, L. H., Li, G., Yang, K., and Jin, R. C. (2016). Integrating plasmonic Au nanorods with dendritic like $\alpha\text{-}Bi_2O_3/Bi_2O_2CO_3$ heterostructures for superior visible-light-driven photocatalysis. *Appl. Catal. B* 184, 1–11. doi: 10.1016/j.apcatb.2015.11.026

Yu, S., Zhang, Y., Dong, F., Li, M., Zhang, T., and Huang, H. (2018). Readily achieving concentration-tunable oxygen vacancies in $Bi_2O_2CO_3$: triple-functional role for efficient visible-light photocatalytic redox performance. *Appl. Catal. B* 226, 441–450. doi: 10.1016/j.apcatb.2017.12.074

Zhang, G. G., Lan, Z. A., and Wang, X. C. (2016). Conjugated polymers: catalysts for photocatalytic hydrogen evolution. *Angew. Chem. Int. Ed.* 55, 15712–15727. doi: 10.1002/anie.201607375

Zhang, J., and Ma, Z. (2017). Enhanced visible-light photocatalytic performance of Ag_3VO_4/Bi_2WO_6 heterojunctions in removing aqueous dyes and tetracycline hydrochloride. *J. Taiwan Inst. Chem. Eng.* 78, 212–218. doi: 10.1016/j.jtice.2017.06.002

Zhang, L., Zhang, Q., Xie, H., Guo, J., Lyu, H., Li, Y., et al. (2017). Electrospun titania nanofibers segregated by graphene oxide for improved visible light photocatalysis. *Appl. Catal. B* 201, 470–478. doi: 10.1016/j.apcatb.2016.08.056

Zhao, T. Y., Zai, J. T., Xu, M., Zou, Q., Su, Y. Z., Wang, K. X., et al. (2011). Hierarchical $Bi_2O_2CO_3$ microspheres with improved visible-light-driven photocatalytic activity. *CrystEngComm* 13:4010. doi: 10.1039/c1ce05113j

Zhong, Y., Liu, Y., Wu, S., Zhu, Y., Chen, H., Yu, X., et al. (2018). Facile fabrication of BiOI/BiOCl immobilized films with improved visible light photocatalytic performance. *Front. Chem.* 6:58. doi: 10.3389/fchem.2018.00058

Zhu, S. S., and Wang, D. W. (2017). Photocatalysis: basic principles, diverse forms of implementations and emerging scientifc opportunities. *Adv. Energy Mater.* 7:1700841. doi: 10.1002/aenm.201700841

Conflict of Interest Statement: The authors declare that the research was conducted in the absence of any commercial or financial relationships that could be construed as a potential conflict of interest.